

Research Article

Dye wastewater treatment with rice husk-derived silica xerogel: An eco-friendly process

Adisak Jaturapiree

Research Center of Natural Materials and Products, Chemistry Program, Faculty of Science and Technology, Nakhon Pathom Rajabhat University, Muang, Nakhon Pathom, 73000 Thailand

Kanjarat Sukrat

Research Center of Natural Materials and Products, Chemistry Program, Faculty of Science and Technology, Nakhon Pathom Rajabhat University, Muang, Nakhon Pathom, 73000 Thailand

Ekrachan Chaichana

Research Center of Natural Materials and Products, Chemistry Program, Faculty of Science and Technology, Nakhon Pathom Rajabhat University, Muang, Nakhon Pathom, 73000 Thailand

Rungtiwa Chidthong

Research Center of Natural Materials and Products, Chemistry Program, Faculty of Science and Technology, Nakhon Pathom Rajabhat University, Muang, Nakhon Pathom, 73000 Thailand

Thanunya Saowapark*

Research Center of Natural Materials and Products, Chemistry Program, Faculty of Science and Technology, Nakhon Pathom Rajabhat University, Muang, Nakhon Pathom, 73000 Thailand

*Corresponding author, E-mail: thanunya@webmail.npru.ac.th

Article Info

<https://doi.org/10.31018/jans.v16i3.5805>

Received: May 25, 2024

Revised: August 13, 2024

Accepted: August 19, 2024

How to Cite

Jaturapiree, A. *et al.* (2024). Dye wastewater treatment with rice husk-derived silica xerogel: An eco-friendly process. *Journal of Applied and Natural Science*, 16(3), 1213 - 1221. <https://doi.org/10.31018/jans.v16i3.5805>

Abstract

Removal of dye contamination from wastewater is crucial for protecting human health and the environment, and adsorption is considered an effective removal method. In addition, agricultural residues are attractive for use as adsorbents for the adsorption due to their renewability. Therefore, the present work aimed to develop silica xerogel from rice husk (agricultural residue in rice production) into an adsorbent for dye wastewater treatment. In the xerogel synthesis, a non-toxic organic acid (citric acid) was used instead of a toxic inorganic acid for leaching and precipitation steps to lower the environmental impact of the process. It was found that the obtained silica xerogel has physical properties such as a surface area and pore volume, comparable with silica xerogels in other literature. When applying it in the dye (methylene blue) wastewater treatment, the obtained silica xerogel showed better adsorption capacity than unprocessed silica at all studied conditions, i.e. various times, pH and initial concentration. The maximum adsorption capacity of the xerogel and unprocessed silica were 103.45 and 61.78 mg/g, respectively. This indicates the benefit of silica xerogel with low environmental impact when applied in dye wastewater treatment. The adsorption isotherms and kinetic for both types of silica were also conducted. It was found that the adsorption process of methylene blue on the silica fitted the Langmuir adsorption isotherm and followed the pseudo-second-order kinetic model. This provides valuable information for optimizing the operating parameters for best performance in a given situation.

Keywords: Adsorption isotherm, Adsorption kinetic, Dry wastewater, Methylene blue, Silica xerogel

INTRODUCTION

Synthetic dyes widely used in many industries, such as paper, textile, food, and pharmaceutical industries, generate wastewater (containing up to 10% of used dye),

which can cause adverse effects on aquatic life and human health (Bawa *et al.*, 2023; Forgacs *et al.*, 2004; Gregory *et al.*, 1981). The remaining dye in the industrial effluents must be removed before draining to lower those effects. Adsorption is considered one of the most

effective and accepted removal methods because it is cheap, renewable and easily available. A variety of materials have been used as an adsorbent, such as biomass (Aragaw *et al.*, 2021), activated carbon (Husien *et al.*, 2022), inorganic materials (Gupta *et al.*, 2009; Kasbaji *et al.*, 2023), and nanomaterial (Ruan *et al.*, 2019).

Biomass, particularly agricultural residues, is very attractive for use due to its renewability and ability to lower its environmental impact. Silica (SiO₂), biomass's most abundant inorganic component, is usually extracted and employed for adsorption (Chen *et al.*, 2022). Silica gel is an amorphous and porous form of silica, consisting of an irregular tridimensional framework of alternating silicon and oxygen atoms with nanometer-scale voids and pores. When the void of silica gel contains gas or vacuum, it is properly called silica xerogel (Henisch, 1988). With many benefits of silica xerogel such as absorbing water readily, high pore volume and surface area, low cost and low energy production, silica xerogel is usually applied as adsorbents (Guzel Kaya *et al.*, 2019).

Synthesis of silica xerogels from agricultural residues have been studied, including rice husk (Kalapathy *et al.*, 2000; Omatolaa *et al.*, 2023), sugarcane bagasse (Affandi *et al.*, 2009), sugarcane leave (Maseko *et al.*, 2023)] and corn husk (Dahliyanti *et al.*, 2022). Nevertheless, most processes to obtain silica xerogel use toxic acids, e.g. hydrochloric acid (HCl) and sulfuric acid (H₂SO₄) during the acid leaching for contaminant removal in the biomass. To reduce the environmental issues of the processes, non-toxic acids should be used instead.

Therefore, the present work aimed to develop silica xerogel from rice husk into an adsorbent for dye wastewater treatment through the eco-friendly process using citric acid C₆H₈O₇ (non-toxic acid). The obtained silica xerogel was evaluated for its adsorption capacity and adsorption characteristics from the adsorption process with methylene blue, represented as a dye pollutant in the wastewater.

MATERIALS AND METHODS

Material

Rice husk, high-content silica biomass (up to 97%) (Nzereogu *et al.*, 2023), was used as silica precursor in silica production. It was collected from a rice processing factory in Ratchaburi province, Thailand. Analytical grade chemicals, i.e. citric acid, sodium hydroxide and ethanol were obtained from Merck. Methylene blue was supplied by the RFCL Limited Co., Ltd.

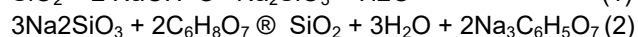
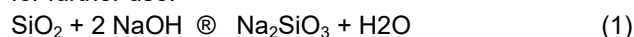
Silica extraction

Rice husk was washed several times with tap water and dried overnight at 70°C. After that, acid leaching was

applied to rice husk to remove metal impurities and decompose organic substances. About 65 g of rice husk was immersed and stirred in 1000 ml of 1 M citric acid at 85°C for 1 hr. The rice husk was separated from acid solution by settling and filtration. Then, acid retained in rice husk was removed by washing with distillation water before drying at 70°C overnight in an Electric oven. The rice husk was then calcined at 700°C using a muffle furnace for 5 hrs. The obtained white powder, designated as rice husk ash (RHA) was milled with mortar and kept in a desiccator before use.

Silica xerogel synthesis

The silica xerogel synthesis was adapted according to the report by Maseko *et al.* (Maseko *et al.*, 2023). At first, 20 g of RSA was reacted with 2.5 M NaOH at 80°C for 2 hr under reflux condenser and vigorous stirring, and sodium silicate (Na₂SiO₃) was then obtained as reaction 1. The obtained sodium silicate was then filtered and stirred for 1 hr. Citric acid was added to the solution with constant stirring until the solution became turbid around pH 7.5-8.5. The solution was gradually converted into the soft gel and after that was aged for 24 hrs. The gel was washed many times with hot water to ensure that the salt content was sodium citrate salt (Na₃C₆H₅O₇) and acid free, as in reaction 2. Ethanol was poured into the gel, kept overnight, and dried at 80°C for 24 hrs. The obtained material designated as rice husk ash xerogel (RHAX) was kept in a desiccator for further use.



Characterization of adsorbent

The surface functional groups of RHA and RHAX were detected by Fourier transform infrared (FTIR) spectroscope (FTIR-2000, PerkinElmer). The spectra were recorded from 4000 to 400 cm⁻¹. The crystalline structure of the samples were analyzed by X-ray diffraction, XRD (Aris, PANalytical) with the Cu-Kα radiation, operating at 40 kV and 40 mA with the scanning rate in 2θ range of 10°–80°. The surface morphology of samples was imaged using a scanning electron microscope (MIRA3, Tescan). The samples were coated with tungsten before being imaged. Surface area and pore structure of the samples were measured by nitrogen adsorption at -196 °C by the surface area analyzer (Quantachrome, USA) before measurement. The sample was degassed at 150°C for 4 hrs.

Batch adsorption studies

Batch adsorption experiments were conducted by adding 0.1 g of an adsorbent into a 250 mL Erlenmeyer flask containing 50 mL of dye solution and then shaking in an incubator at 120 rpm at 30°C for 24 hrs. After shaking, the adsorbent was separated from the solution

by filtration and centrifugation. The concentrations of dye solution were determined by absorbance measurement using a beam UV Vis spectrophotometer at 664 nm. They were then calculated using the standard calibration curves. The percentage of dye removal and the adsorption capacity, q (mg of dye /g of adsorbent) were calculated using Equation 1,

$$q_e = \frac{C_0 - C_e}{m} V \quad \text{Eq.1}$$

where C_0 and C_e represent the concentration of dye (mg/L) in the solution at time, $t = 0$ and at any time, t , respectively. V is the volume of solution (L) and m is the amount of adsorbent used (g).

The effects of contact time and MB initial concentrations were studied in the range of 0 – 24 h, and 50-400 mg/L. The effect of pH was studied in the range of 2-13 and the pH was adjusted with 0.1 M NaOH and 0.1M HCl solutions. The adsorption isotherms were performed at different initial concentrations of MB between 25-200 mg/L. The adsorption kinetic was studied using MB initial concentrations of 150 mg/L at contact time from 0-2 hrs.

RESULTS AND DISCUSSION

Characterization of adsorbent

The XRD patterns of RHA and RHAX are shown in Fig. 1. It was found that both patterns were similar, suggesting that there were no changes in crystal structure inside the silica during the gelation process. They similarly showed strong, broad diffraction peaks at around $2\theta = 22-24^\circ$, which is assigned to the characteristic of amorphous SiO_2 structure as reported earlier (Affandi *et al.*, 2009; Kalapathy *et al.*, 2000).

FTIR characterization was carried out to examine the functional group characteristics of RHA and RHAX, as shown in Fig. 2. The FTIR spectra of both samples exhibited the same vibration patterns, indicating that the gelation process does not alter the functional groups of the silica. The peaks at 1055 and 800 cm^{-1} are assigned to the Si-O stretching vibration in Si-O-Si bonds, and the peak appearing at 460 cm^{-1} corresponds to the bending vibration of Si-O-Si (Dahliyanti *et al.*, 2022; Maseko *et al.*, 2023).

The SEM images of RHA and RHAX at various magnifications are presented in Fig. 3. It can be seen that the surface of RHA was compact and smooth and exhibited a non-porous structure. On the contrary, the surface of RHAX was rough with a porous structure. Agglomeration form of nearly spherical particles can be observed in the RHAX structure. This is a general microstructure of silica xerogel, as observed in previous literature (Dorairaj *et al.*, 2022; Vander Auwera *et al.*, 2013).

The surface area, pore volume, and pore diameter of RHA and RHAX are presented in Table 1. All men-

tioned parameters of RHAX were higher than those of RHA. This is a benefit of xerogel which enhances the properties of typical silica to be suitable for application in various applications, particularly adsorption processes. Compared with silica xerogel from other literature, the surface area of the xerogel produced in this study is still in the range ($122-668 \text{ m}^2/\text{g}$) (Affandi *et al.*, 2009; Arenas *et al.*, 2007; Dahliyanti *et al.*, 2022; Maseko *et al.*, 2023; Omatolaa *et al.*, 2023). The differences in the silica sources and production procedures could lead to different properties of the obtained xerogel.

Adsorption properties

The adsorption capacities of the samples were evaluated with dye (methylene blue, MB) with an initial concentration of 150 mg/L on 0.1 g of the adsorbent at 30°C for 15-240 min, and are shown in Fig. 4. Methylene blue is a cationic dye widely used in the textile industrial. The process parameters for methylene blue have been studied so far with various adsorbents (Allahkarami *et al.*, 2024; Gherraby *et al.*, 2024). From the experiments, it was found that the adsorption capacity of RHA and RHAX toward MB gradually increased at the beginning of contact time and then remained constant. The equilibrium time observed for RHA and RHAX were 80 and 120 min, respectively. RHAX showed higher adsorption capacities than RHA for all contact times studied. The highest adsorption capacity of RHAX was about 1.4 times greater than that of RHA, which much more than the ratio of surface areas between two materials (1.04 times). This indicates that other factors affected the adsorption capacity of these adsorbents more than the surface area. The larger pore size and pore volume of RHAX may be the main reason for enhancing the adsorption capacity of the large molecule substance (MB) onto the surface. In addition, more active sites may be available on the xerogel, and they can be easily accessed due to the larger pore size (Ahmad *et al.*, 2014).

The effect of initial pH of the dye solution on the adsorption capacity was studied by varying the initial pH in the ranges of 2–11 under constant process parameters (150 mg/L of MB initial concentration, 0.10 g of the adsorbents and at 30°C). The result of the study is shown in Fig. 5. It can be seen that the adsorption capacity increases with pH until it is constant around pH above 7, indicating a basic solution. This could be reasoned from that at basic condition, the adsorbent surface became negatively charged due to deprotonation and would be more attracted to the positive charges of MB (cationic dyes) and then increased the adsorption capacity (Khan *et al.*, 2016; Kushwaha *et al.*, 2014). Nevertheless, RHAX still had higher adsorption capacities than RHA for all pH ranges. In fact, the pH of MB solution in the study had already been about 6-7. Therefore, the best adsorption condition can be ob-

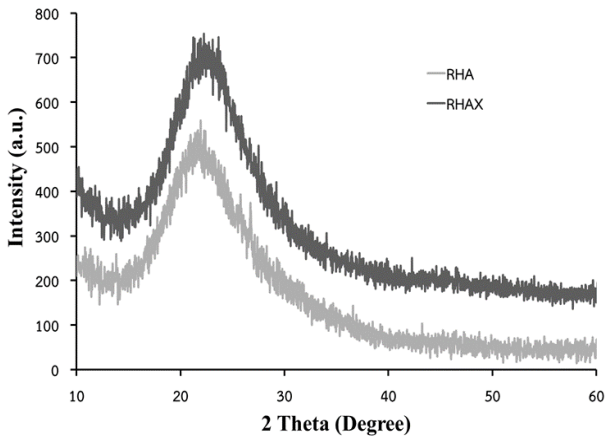


Fig. 1. X-Ray diffraction patterns of the adsorbents

tained without adjusting the pH of MB solution. In addition, the actual wastewater generally has a neutral pH around 6-7. Hence, there was no need for pH adjustment for the rest of this study, and the pH was then spontaneously constant at around 6-7.

The effect of MB initial concentration was studied between 25–250 mg/L for 4 h at which the full equilibrium was attained, and the results are presented in Fig. 6. The adsorption capacity increased from 12.37 to 61.78 mg/g for RHA, and from 12.44 to 103.45 mg/g for RHAX. RHA reached the highest adsorption capacity at the lower initial concentration than RHAX. It suggests that RHAX has the higher active sites, and is still available for adsorption, even at the high initial concentration. In addition, for both adsorbents the higher concentration gradient could act as a driving force to overcome all mass transfer resistance for the adsorption process and give the higher adsorption capacity (Foo *et al.*, 2012; Khan *et al.*, 2016).

Adsorption isotherm

Adsorption isotherm is a mathematical model of adsorption process, which describes the interaction between adsorbates and adsorbents. In this experiment, three well-known models i.e. Langmuir, Freundlich, and Temkin isotherms were used to describe the adsorption process.

The Langmuir isotherm (Langmuir, 1918) is expressed based on the assumption of monolayer coverage of dyes onto a homogeneous surface of the adsorbent. The linear equation of Langmuir adsorption is represented as Equation 2,

$$\frac{C_e}{q_e} = \frac{1}{q_m K_L} + \frac{C_e}{q_m} \tag{Eq.2}$$

where C_e is the equilibrium concentration of the dye (mg/l), q_e is the amount of dye adsorbed per unit mass of adsorbent (mg/g), q_m is the maximum adsorption capacity (mg/g), and K_L is Langmuir constant (L/mg). The q_m and K_L can be calculated from the intercept and

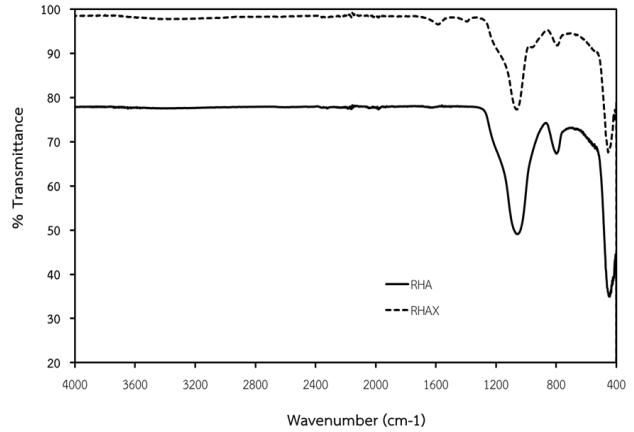


Fig. 2. Fourier transform Infrared spectroscopy spectra of the adsorbents

slope of a linear plot of C_e/q_e versus C_e , as shown in Fig. 7.

The essential characteristics of the Langmuir isotherm can be expressed in terms of a dimensionless constant called equilibrium parameter (R_L), which can be described for the reversibility of the adsorption process, defined as Equation 3,

$$R_L = \frac{1}{1 + K_L C_0} \tag{Eq.3}$$

where K_L is the Langmuir constant and C_0 is the initial concentration of dye (mg/L). R_L is equilibrium parameter. If the type of isotherm to be irreversible ($R_L = 0$), favorable ($0 < R_L < 1$), linear ($R_L = 1$) or unfavorable ($R_L > 1$). 12

The Freundlich isotherm (Freundlich, 1906) is derived based on the assumptions of the adsorption characteristics of multilayer and heterogeneous surfaces. The nonlinear equation of Freundlich adsorption is represented as Equation 4,

$$\log q_e = 1/n \log C_e + \log K_F \tag{Eq. 4}$$

where C_e and q_e are defined similarly in the Langmuir equation, K_F and $1/n$ are Freundlich constants related to adsorption capacity and adsorption intensity of the sorbent, respectively, which are calculated from the intercept and slope of a linear plot of $\log q_e$ versus $\log C_e$ (Fig. 7).

The Temkin isotherm model is based on the change of the adsorption heat in the adsorptive layer. It can be expressed by the linear equation as Equation 5 and 6 (Temkin *et al.*, 1940),

$$q_e = B \ln A_T + B \ln C_e \tag{Eq. 5}$$

$$B = RT/b_T \tag{Eq.6}$$

where A_t is the Temkin isotherm constant (L/mg), b_T is the Temkin isotherm constant, B is constant related to heat of sorption (J/mol), R is the universal gas constant (8.314 J/mol.K), T is the absolute temperature (K), and B , A_T , b_T can be calculated from slope and intercept of a linear plot of q_e versus $\ln C_e$ (Fig. 7).

Table 1. Surface areas and pore characteristics of the adsorbents

Sample	Surface area (m ² /g)	Total pore volume (cm ³ /g)	Pore size (nm)
RHA	189	0.240	5.31
RHAX	197	0.556	11.27

RHA: rice husk ash; RHAX: rice husk ash xerogel

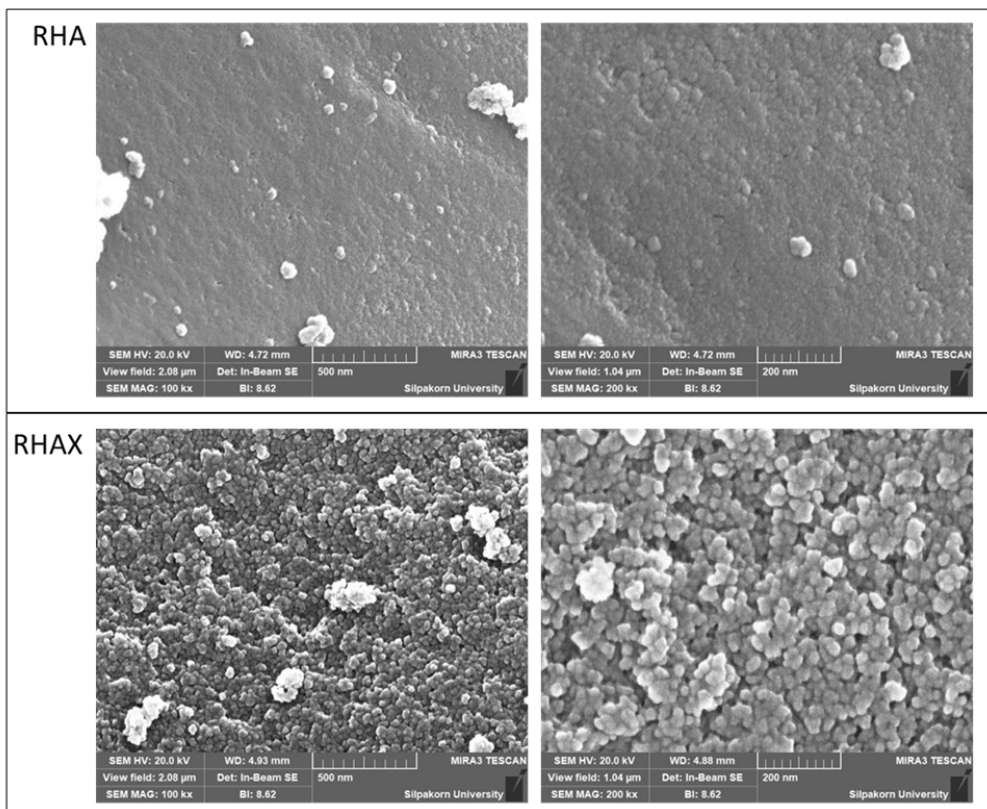


Fig. 3. Scanning electron microscope images of the adsorbents. Showing that RHA surface was compact and smooth with a non-porous structure, while RHAX surface was rough with a porous structure and particle agglomeration

All experimental data for the adsorption of MB onto RHA and RHAX as presented in Fig. 7 can be extracted for the corresponding parameters of all the three isotherms, shown in Table 2.

Considering R^2 and Δq_e values of RHA and RHAX, it can be seen that the Langmuir isotherm has a higher value of R^2 (0.9892) and a lower value of Δq_e (6.549), compared with the Freundlich and Temkin isotherms. This suggests that the Langmuir model could better fit the adsorption processes of both adsorbents than the other models. The R_L values for RHA and RHAX were found to be 0.0036 and 0.0492, greater than 0 but less than 1, indicating that Langmuir isotherm is favourable (Vargas *et al.*, 2011). The maximum monolayer coverage capacity (q_m) of RHAX (106.38 mg/g) is much larger than that of RHA (59.52 mg/g), beneficial from a xerogel structure with more surface roughness and higher pore volume. Similar results have been reported with various types of silica (Dahliyanti *et al.*, 2022; Guzel Kaya *et al.*, 2019; Juzsakova *et al.*, 2023). However, silica xerogel from the present study exhibited

higher removal capacity than the others.

Nevertheless, it is known that in one adsorption process, many adsorption types could occur simultaneously. Thus, Freundlich and Temkin are still useful for describing the adsorption characteristics of the adsorption process with acceptable R^2 values as observed.

The n parameter in the Freundlich model, known as the heterogeneity factor, can be used to describe important information about adsorption systems. If n is in the range of 2-10, indicating good adsorption, 1-2 moderate adsorption and less than one denoted poor adsorption (Shang *et al.*, 2014). From the result, the n values of both adsorbents were higher than 2, indicating effective adsorbents for MB adsorption process.

The Temkin isotherm can be used to identify the two main types of adsorption, i.e. physisorption and chemisorption, by measuring the heat of adsorption "B value". Physisorption occurs if B is less than 1.0 kcal/mol, and chemisorption occurs if B is more than 20 kcal/mol. Both of the adsorption types occur with B between 1 and 20. For RHA and RHAX, their B values (7.97 and

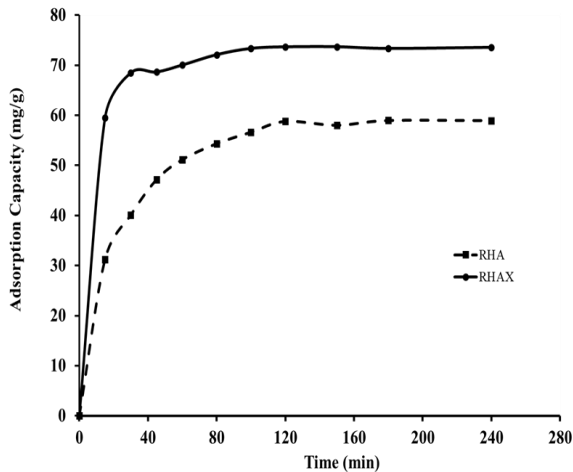


Fig. 4. Adsorption capacity of the adsorbents at various times

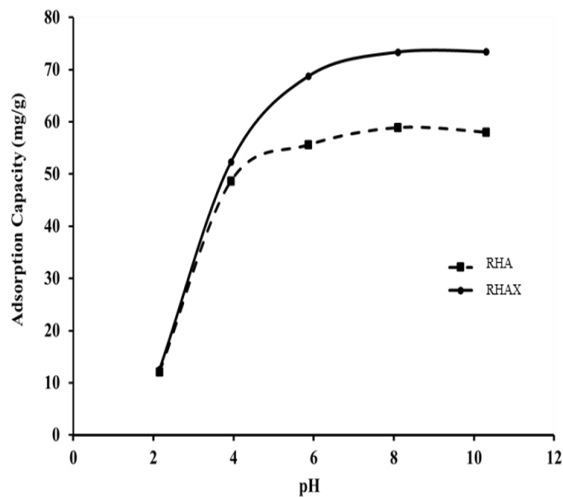


Fig. 5. Adsorption capacity of the adsorbents at various initial pH of the solution

19.13) are between 1 and 20, pointing out that the adsorption processes involve both physisorption and chemisorption (Mohamed *et al.*, 2022). In addition, the positive values of *b* also indicate to an exothermic reaction during the adsorption (Hamdaoui, 2006).

Adsorption kinetic

Two simplified kinetic models, including the pseudo-first order (Lagergren, 1898) and pseudo-second order kinetic models (Ho *et al.*, 1999) were used here to understand the adsorption mechanism influenced by chemical reaction rates and mass transfer.

The pseudo-first-order kinetics is expressed in a linear form as Equation 7.

$$\ln(q_e - q_t) = \ln q_e - k_1 t \tag{Eq.7}$$

Where q_e and q_t are the amount of MB adsorbed (mol g^{-1}) at equilibrium and at time t (min), respectively, k_1 is the rate constant of adsorption (min^{-1}), k_1 value was calculated from the plots of $\ln(q_e - q_t)$ versus t at different concentrations.

The pseudo-second-order kinetics is expressed in a

Table 2. Isotherm parameters for the adsorption of methylene blue on the adsorbents

Isotherm	Parameters	RHA	RHAX
Langmuir	q_m (mg/g)	59.52	106.38
	K_L (L/mg)	1.05	1.807
	R_L	0.0064	0.0036
	R^2	0.9922	0.9952
	Δq_e (%)	3.197	3.776
Freundlich	K_F (L/g)	31.62	57.16
	n	5.714	2.798
	R^2	0.8632	0.9284
Temkin	Δq_e (%)	18.64	13.03
	A_T	81.13	23.38
	b	7.3761	19.13
	R^2	0.9144	0.9813
	Δq_e (%)	8.774	6.058

q_m : maximum adsorption capacity; K_L : Langmuir constant, R_L : equilibrium parameter;

R^2 : coefficient of determination, Δq_e (%): value of normalized standard deviation;

K_F : Freundlich constant, n : adsorption intensity of the adsorbents; A_T : Temkin isotherm equilibrium binding constant, b : Temkin constant related to heat of sorption

Table 3. Adsorption kinetics parameters of methylene blue on the adsorbents

Reaction	Parameters	RHA	RHAX
Pseudo-first order	$q_{e, cal}$	18.45	16.69
	k_1	0.0104	0.0032
	R^2	0.765	0.606
Pseudo-second order	Δq_e (%)	68.80	79.94
	$q_{e, cal}$	59.88	74.62
	k_1	0.0014	0.0042
	R^2	0.9986	0.9998
	Δq_e (%)	1.21	10.34

$q_{e, cal}$: the amount of methylene blue adsorbed onto the adsorbents at equilibrium;

k_1 : rate constant of adsorption, R^2 : coefficient of determination; Δq_e (%): value of normalized standard deviation

linear form as Equation 8.

$$\frac{t}{q_t} = \frac{1}{k_2 q_e^2} + \frac{t}{q_e} \tag{Eq.8}$$

Eq.8

where k_2 is the rate constant of the pseudo-second-order adsorption ($\text{g.mol}^{-1} \text{min}^{-1}$), k_2 value and q_e were

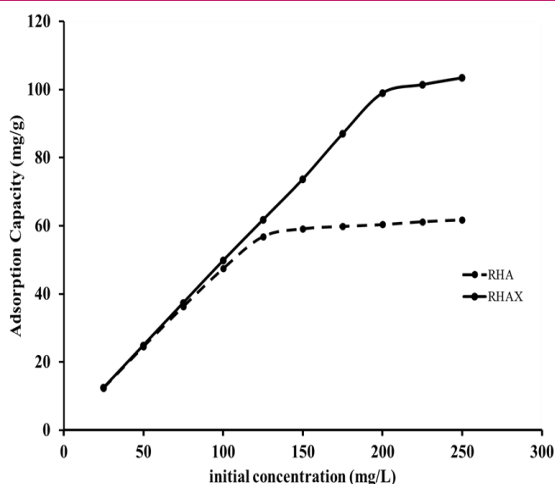


Fig. 6. Adsorption capacity of the adsorbents at various initial concentration of the solution

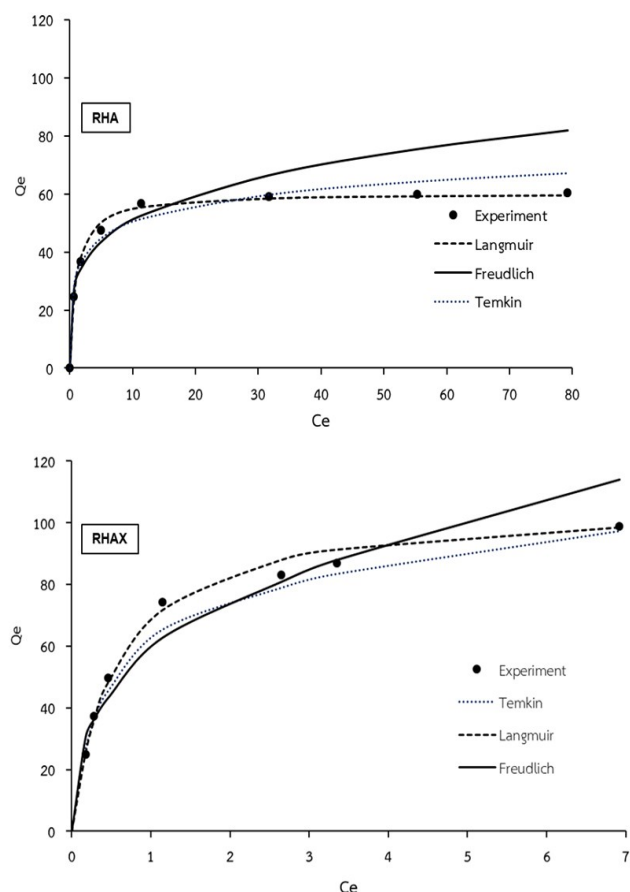


Fig. 7. Various adsorption isotherms of the adsorbents

calculated from the intercept and slope of the plots of t/q_t versus t at different concentrations.

All kinetic parameters of both reaction types are shown in Table 3. It was seen that the correlation coefficient (R^2) of the pseudo-second-order model for both RHA and RHAX (0.9986 and 0.9998) were closer to unity than those for the pseudo-first-order model (0.765 and 0.606). The value of normalized standard deviation Δq (%) of the pseudo-second-order model was also lower

than that of the the pseudo-first-order model. It can be concluded that the kinetics of MB adsorption on RHA and RHAX followed a pseudo-second-order model, which could imply that the chemisorption process involved in the adsorption process (Cherifi *et al.*, 2013; Islam *et al.*, 2017). The electrostatic attraction between negative charges on the surface of both silica and the positive charges of cationic dye (MB) may play an important role in adsorption. A similar model was observed for adsorption of methylene blue onto many types of silica (Kushwaha *et al.*, 2014; Li *et al.*, 2020).

Conclusion

Silica xerogel can be synthesized here using biomass precursor in an eco-friendly process with a nontoxic organic acid (citric acid) presence. The obtained silica xerogel has better physical properties than the normal silica. The methylene blue adsorption capability was also found that the silica xerogel had a higher adsorption capacity than the normal silica at all conditions, i.e. various time, pH, and initial concentrations. This suggests that this low-environmental impact silica xerogel can be a potential cost-effective adsorbent for dye removal in wastewater treatment processes. The adsorption process of MB for both types of silica fitted the Langmuir adsorption isotherm and followed the pseudo-second-order kinetic model. This provides valuable information for optimizing the operating parameters for best performance in a given situation.

ACKNOWLEDGEMENTS

The authors thank Thailand Science Research and Innovation (TSRI) for the financial support for this project.

Conflict of interest

The authors declare that they have no conflict of interest.

REFERENCES

- Affandi, S., Setyawan, H., Winardi, S., Purwanto, A. & Balgis, R. (2009). A facile method for production of high-purity silica xerogels from bagasse ash. *Advanced Powder Technology*, 20(5), 468-472. DOI: 10.1016/j.appt.2009.03.008
- Ahmad, M. A., Ahmad Puad, N. A. & Bello, O. S. (2014). Kinetic, equilibrium and thermodynamic studies of synthetic dye removal using pomegranate peel activated carbon prepared by microwave-induced KOH activation. *Water Resources and Industry*, 6, 18-35. DOI: 10.1016/j.wri.2014.06.002
- Allahkarami, E., Allahkarami, E., Heydari, M., Azadmehr, A. & Maghsoudi, A. (2024). Assessment of chromite ore wastes for methylene blue adsorption: Isotherm, kinetic,

- thermodynamic studies, ANN, and statistical physics modeling. *Chemosphere*, 358, 142098. DOI: 10.1016/j.chemosphere.2024.142098
4. Aragaw, T. A. & Bogale, F. M. (2021). Biomass-Based Adsorbents for Removal of Dyes From Wastewater: A Review. *Frontiers in Environmental Science*, 9. DOI: 10.3389/fenvs.2021.764958
 5. Arenas, L., Simm, C., Gushikem, Y., Dias, S., Moro, C., Costa, T. & Benvenuti, E. (2007). Synthesis of silica xerogels with high surface area using acetic acid as catalyst. *Journal of The Brazilian Chemical Society - JBCS*, 18. DOI: 10.1590/S0103-50532007000500003
 6. Bawa, I., Irdhawati & Putri, K. (2023). Combined adsorbent of corn husks and eggshells activated by sodium hydroxide as an adsorbent for Remazol Yellow FG dye in textile waste. *Journal of Applied and Natural Science*, 15, 1582-1586. DOI: 10.31018/jans.v15i4.5124
 7. Chen, K., Ng, K. H., Cheng, C. K., Cheng, Y. W., Chong, C. C., Vo, D.-V. N., Witoon, T. & Ismail, M. H. (2022). Biomass-derived carbon-based and silica-based materials for catalytic and adsorptive applications- An update since 2010. *Chemosphere*, 287, 132222. DOI: 10.1016/j.chemosphere.2021.132222
 8. Cherifi, H., Fatiha, B. & Salah, H. (2013). Kinetic studies on the adsorption of methylene blue onto vegetal fiber activated carbons. *Applied Surface Science*, 282, 52-59. DOI: 10.1016/j.apsusc.2013.05.031
 9. Dahliyanti, A., Yunitama, D. A., Rofiqoh, I. & Mustapha, M. (2022). Synthesis and characterization of silica xerogel from corn husk waste as cationic dyes adsorbent. *F1000Research*, 11, 305. DOI: 10.12688/f1000research.75979.1
 10. Dorairaj, D., Govender, N., Zakaria, S. & Wickneswari, R. (2022). Green synthesis and characterization of UKMRC-8 rice husk-derived mesoporous silica nanoparticle for agricultural application. *Scientific Reports*, 12(1), 20162. DOI: 10.1038/s41598-022-24484-z
 11. Foo, K. Y. & Hameed, B. H. (2012). Mesoporous activated carbon from wood sawdust by K₂CO₃ activation using microwave heating. *Bioresource technology*, 111, 425-432. DOI: 10.1016/j.biortech.2012.01.141
 12. Forgacs, E., Cserh ati, T. & Oros, G. (2004). Removal of synthetic dyes from wastewaters: a review. *Environment International*, 30(7), 953-971. DOI: 10.1016/j.envint.2004.02.001
 13. Freundlich, H. (1906). Over the adsorption in solution. *International Journal of Research in Physical Chemistry and Chemical Physics*, 57, 387-470.
 14. Gherraby, Y., Rachdi, Y., El Alouani, M., Aouan, B., Basam, R., Cherouaki, R., Saufi, H., Khouya, E. h. & Belaouad, S. (2024). Application of Aptenia cordifolia powder as a biosorbent for methylene blue retention from an aqueous medium: Isotherm, kinetic, and thermodynamic investigations. *Desalination and Water Treatment*, 318, 100263. DOI: 10.1016/j.dwt.2024.100263
 15. Gregory, A. R., Elliott, J. & Kluge, P. (1981). Ames testing of direct black 38 parallels carcinogenicity testing. *Journal of Applied Toxicology*, 1(6), 308-313. DOI: 10.1002/jat.2550010608
 16. Gupta, V. K. & Suhas. (2009). Application of low-cost adsorbents for dye removal--a review. *J Environ Manage*, 90 (8), 2313-2342. DOI: 10.1016/j.jenvman.2008.11.017
 17. Guzel Kaya, G., Yilmaz, E. & Deveci, H. (2019). A novel silica xerogel synthesized from volcanic tuff as an adsorbent for high-efficient removal of methylene blue: parameter optimization using Taguchi experimental design. *Journal of Chemical Technology & Biotechnology*, 94(8), 2729-2737. DOI: 10.1002/jctb.6089
 18. Hamdaoui, O. (2006). Batch study of liquid-phase adsorption of methylene blue using cedar sawdust and crushed brick. *Journal of hazardous materials*, 135(1), 264-273. DOI: 10.1016/j.jhazmat.2005.11.062
 19. Henisch, H. K. (1988). *Crystals in Gels and Liesegang Rings*: Cambridge University Press.
 20. Ho, Y. S. & McKay, G. (1999). Pseudo-second order model for sorption processes. *Process biochemistry*, 34(5), 451-465. DOI: 10.1016/S0032-9592(98)00112-5
 21. Husien, S., El-taweel, R., Salim, A., Fahim, I., Said, L. & Radwan, A. (2022). Review of activated carbon adsorbent material for textile dyes removal: Preparation, and modeling. *Current Research in Green and Sustainable Chemistry*, 5, 100325. DOI: 10.1016/j.crgsc.2022.100325
 22. Islam, M. A., Ahmed, M. J., Khanday, W. A., Asif, M. & Hameed, B. H. (2017). Mesoporous activated carbon prepared from NaOH activation of rattan (*Lacosperma secundiflorum*) hydrochar for methylene blue removal. *Ecotoxicology and Environmental Safety*, 138, 279-285. DOI: 10.1016/j.ecoenv.2017.01.010
 23. Juzsakova, T., Salman, A. D., Abdullah, T. A., Rasheed, R. T., Zsirka, B., Al-Shaikhly, R. R., Sluser, B. & Cretescu, I. (2023). Removal of Methylene Blue from Aqueous Solution by Mixture of Reused Silica Gel Desiccant and Natural Sand or Eggshell Waste. *Materials*, 16(4), 1618.
 24. Kalapathy, U., Proctor, A. & Shultz, J. (2000). A simple method for production of pure silica from rice hull ash. *Bioresource technology*, 73(3), 257-262. DOI: 10.1016/S0960-8524(99)00127-3
 25. Kasbaji, M., Ibrahim, I., Mennani, M., Abdelatty abuelalla, O., fekry, S. S., Mohamed, M. M., Salama, T. M., Moneam, I. A., Mbarki, M., Moubarik, A. & Oubenali, M. (2023). Future trends in dye removal by metal oxides and their Nano/Composites: A comprehensive review. *Inorganic Chemistry Communications*, 158, 111546. DOI: 10.1016/j.inoche.2023.111546
 26. Khan, T. A., Khan, E. A. & Shahjahan. (2016). Adsorptive uptake of basic dyes from aqueous solution by novel brown linseed deoiled cake activated carbon: Equilibrium isotherms and dynamics. *Journal of Environmental Chemical Engineering*, 4(3), 3084-3095. DOI: 10.1016/j.jece.2016.06.009
 27. Kushwaha, A. K., Gupta, N. & Chattopadhyaya, M. C. (2014). Enhanced adsorption of methylene blue on modified silica gel: equilibrium, kinetic, and thermodynamic studies. *Desalination and Water Treatment*, 52(22-24), 4527-4537. DOI: 10.1080/19443994.2013.803319
 28. Lagergren, S. (1898). Zur Theorie der Sogenannten Adsorption Gel oster Stoffe, Kungliga Svenska Vetenskapssakademiens. *Handlingar*, 24(4), 1-39.
 29. Langmuir, I. (1918). The adsorption of gases on plane surfaces of glass, mica and platinum. *Journal of the American Chemical Society*, 40(9), 1361-1403.
 30. Li, Y., Wang, S., Shen, Z., Li, X., Zhou, Q., Sun, Y., Wang, T., Liu, Y. & Gao, Q. (2020). Gradient Adsorption of Methylene Blue and Crystal Violet onto Compound Mi-

- roporous Silica from Aqueous Medium. *ACS Omega*, 5 (43), 28382-28392. DOI: 10.1021/acsomega.0c04437
31. Maseko, N. N., Enke, D., Iwarere, S. A., Oluwafemi, O. S. & Pocock, J. (2023). Synthesis of low density and high purity silica xerogels from south african sugarcane leaves without the usage of a surfactant. *Sustainability*, 15(5), 4626. DOI: 10.3390/su15054626
32. Mohamed, F., Shaban, M., Zaki, S. K., Abd-Elsamie, M. S., Sayed, R., Zayed, M., Khalid, N., Saad, S., Omar, S., Ahmed, A. M., Gerges, A., El-Mageed, H. R. A. & Soliman, N. K. (2022). Activated carbon derived from sugarcane and modified with natural zeolite for efficient adsorption of methylene blue dye: experimentally and theoretically approaches. *Scientific Reports*, 12(1), 18031. DOI: 10.1038/s41598-022-22421-8
33. Nzereogu, P. U., Omah, A. D., Ezema, F. I., Iwuoha, E. I. & Nwanya, A. C. (2023). Silica extraction from rice husk: Comprehensive review and applications. *Hybrid Advances*, 4, 100111. DOI: 10.1016/j.hybadv.2023.100111
34. Omatolaa, K., Onojah, A. & Ahemen, I. (2023). Synthesis and characterization of silica xerogel and aerogel from rice husk ash and pulverized beach sand via sol-gel route. *Journal of the Nigerian Society of Physical Sciences*, 11609. DOI: 10.46481/jnsps.2023.1609
35. Ruan, W., Hu, J., Qi, J., Hou, Y., Zhou, C. & Wei, X. (2019). Removal of dyes from wastewater by nanomaterials : A review. *Advanced Materials Letters*, 10(1), 9-20. DOI: 10.5185/amlett.2019.2148
36. Shang, T. X., Zhang, J., Jin, X. J. & Gao, J. M. (2014). Study of Cr(VI) adsorption onto nitrogen-containing activated carbon preparation from bamboo processing residues. *Journal of Wood Science*, 60(3), 215-224. DOI: 10.1007/s10086-014-1392-4
37. Temkin, M. I. & Pyzhev, V. (1940). Kinetics of ammonia synthesis on promoted iron catalysts. *Acta Physicochim U.R.S.S.*, 12, 217-222.
38. Vander Auwera, J., Ngo, N. H., El Hamzaoui, H., Capoen, B., Bouazaoui, M., Ausset, P., Boulet, C. & Hartmann, J. M. (2013). Infrared absorption by molecular gases as a probe of nanoporous silica xerogel and molecule-surface collisions: Low-pressure results. *Physical Review A*, 88(4), 042506. DOI: 10.1103/PhysRevA.88.042506
39. Vargas, A. M., Cazetta, A. L., Kunita, M. H., Silva, T. L. & Almeida, V. C. (2011). Adsorption of methylene blue on activated carbon produced from flamboyant pods (*Delonix regia*): Study of adsorption isotherms and kinetic models. *Chemical Engineering Journal*, 168(2), 722-730. DOI: 10.1016/j.cej.2011.01.067